EurJIC
European Journal of Inorganic Chemistry

Full Papers
doi.org/10.1002/ejic.202001055

Chemistry Europe
European Chemical Societies Publishing

A "Solvent-Free" Crystal Structure of [Fe{N(SiMe$_3$)$_2$}$_3$] – Synthesis, Structure and Properties

Sylvio Indris,[a] Michael Knapp,[a] Björn Schwarz,[a] and Andreas Eichhöfer*[b, c]

For the synthesis of the ferric bis(trimethylsilyl)amido complex [Fe{N(SiMe$_3$)$_2$}$_3$] literature gives differing synthetic protocols based on crystallization from solution. In this report we present a 'solvent-free' structural phase of [Fe{N(SiMe$_3$)$_2$}$_3$] which was isolated by sublimation of the product obtained from the reaction of 2 eq $FeCl_3$ with 3 eq LiN(SiMe$_3$)$_2$ in benzene. It could be characterized by single crystal as well as powder XRD and elemental analysis. However, ^{57}Fe Mößbauer spectroscopy suggests a contamination of the main product with an Fe(II) species. Also, a part of the solid reaction byproducts from the reactions in solution were identified by powder XRD and ^{7}Li MAS NMR which indicate distinct redox side reactions between oxidizing $FeCl_3$ and reducing LiN(SiMe$_3$)$_2$, a fact which rationalizes the lower than expected yields and the observation of an Fe(II) impurity compound. AC magnetic measurements of [Fe{N(SiMe$_3$)$_2$}$_3$] have been performed in an extended frequency range up to 10^4 s^{-1}, allowing for a more precise evaluation of the magnetic relaxation parameters when compared to previously published measurements.

Introduction

Bis(trimethylsilyl)amido complexes of 1st row transition metals [M{N(SiMe$_3$)$_2$}$_n$] (n = 2, 3) are useful starting compounds in complex chemistry.[1,2,3,4] Investigation of transition metal amides in our laboratory originally stems from the interest to utilize them as precursor complexes for the synthesis of mixed metal chalcogenide cluster complexes[5] and polymeric metal chalcogenolato complexes.[6] Recently, it also turned out that low coordinated metal complexes of type [Fe{N(SiMe$_3$)$_2$}$_2$L] (L = ligand) comprise interesting magnetic properties and can act as useful model complexes for the study of effects in the research area of single ion molecular magnetism.[7,8,9] For compounds with M^{3+} = Sc, Ti, Cr, Fe, syntheses and properties have been described in the sixties and seventies by Bürger and Wannagat[10] as well as Bradley and coworkers.[11,12,13,14] The crystal structures have been determined for many complexes with composition [M{N(SiMe$_3$)$_2$}$_3$] (M^{3+} = Sc,[15,16] Ti,[17] V,[18] Cr,[19] Mn,[20] Fe,[21,22] Co[20]) of the 1st row transition metals. All of them crystallize from solution in the same trigonal space group $P\bar{3}1c$. The packing of the molecules along the crystallographic c axis results in large hexagonal channels, which are often filled with disordered solvent molecules.[21,22] In the case of [Cr{N(SiMe$_3$)$_2$}$_3$] smart utilization of this fact resulted in a crystal structure which is almost free of disorder by cocrystallisation with hexamethyldisilane.[19] Recently also a 'solvent-free' crystal structure type of [Sc{N(SiMe$_3$)$_2$}$_3$] was reported for crystals directly obtained by sublimation.[16]

This work reports the 'solvent-free' crystal structure of the Fe(III) complex [Fe{N(SiMe$_3$)$_2$}$_3$] along with a characterization of the reaction byproduct Li_2FeCl_4 by powder X-ray diffraction (XRD), ^{7}Li magic-angle spinning (MAS) nuclear magnetic resonance (NMR) spectroscopy, and Mößbauer spectroscopy.

Synthesis and Structure

Concerning the synthesis of [Fe{N(SiMe$_3$)$_2$}$_3$] (**1**) four main publications can be found in literature.

Bürger and Wannagat made use of the reaction of $FeCl_3$ and NaN(SiMe$_3$)$_2$ and reported influences of the choice of solvent and stoichiometry of the reaction educts on the product formation.[10] Based on their observations (i.e. the formation of the complex salt Na_4FeCl_6 instead of NaCl as the reaction byproduct) they suggested for the synthesis of **1** the use of a 2:3 reaction stoichiometry (instead of the more obvious 1:3) in toluene as a solvent. Bradley and coworkers originally reported for the synthesis of **1** a 1:3 reaction of $FeCl_3$ and LiN(SiMe$_3$)$_2$ in thf.[11] This protocol was later on refined and changed to a 2:3 reaction stoichiometry in benzene solution resulting in yields of 62%.[23] Lee and coworkers again utilized for the synthesis of **1** the reaction of the sodium salt NaN(SiMe$_3$)$_2$ with 2/3 equivalents of $FeCl_3$ in benzene as a solvent similar to the approach of

[a] Dr. S. Indris, Dr. M. Knapp, Dr. B. Schwarz
Institute for Applied Materials - Energy Storage Systems (IAM-ESS), Karlsruhe Institute of Technology (KIT),
Hermann-von-Helmholtz-Platz 1, 76344 Eggenstein-Leopoldshafen, Germany
[b] Dr. A. Eichhöfer
Institut für Nanotechnologie, Karlsruher Institut für Technologie (KIT), Campus Nord,
Hermann-von-Helmholtz-Platz 1, 76344 Eggenstein-Leopoldshafen, Germany
E-mail: andreas.eichhoefer@kit.edu
[c] Dr. A. Eichhöfer
Karlsruhe Nano Micro Facility (KNMF),
Hermann-von-Helmholtz-Platz 1, 76344 Eggenstein-Leopoldshafen, Germany

Supporting information for this article is available on the WWW under https://doi.org/10.1002/ejic.202001055

Bürger and Wannagat. They reported yields of about 56%, which are 'primarily limited by the high product solubility'.[24] In addition they give two important notes in their paper. First: 'the other synthesis for **1** – the reaction of 1:3 $FeCl_3$/Li[N($SiMe_3$)$_2$] in THF – is not as straightforward as an earlier report of Bradley and coworkers implies'.[11] Instead they found that reactions with a 2:3 stoichiometry in THF resulted in the synthesis of [FeCl(N($SiMe_3$)$_2$)$_2$] in 73% yield. Second: 'the reaction at the limiting stoichiometry of 1:3 $FeCl_3$/Na[N($SiMe_3$)$_2$] gives impurities that are difficult to separate from product'.

1:3 Reaction of $FeCl_3$ and $LiN(SiMe_3)_2$

Despite these findings the synthesis of **1** was also attempted in this work as a first approach with the more intuitive 1:3 ratio of iron(III) chloride and the lithium amide in benzene solution. It turns out that the amount of insoluble reaction product, separated by centrifugation, is slightly larger than calculated for 3 eq. of LiCl (Scheme 1).

The powder XRD pattern of this pale beige powder indeed suggested the formation of a lithium iron(II) chloride salt by comparing the observed pattern with those calculated for e.g. Li_2FeCl_4,[25] $Li_{1.86}Fe_{1.09}Cl_4$[26] and Li_6FeCl_8 (Figure 1).[27] The ^{57}Fe Mößbauer spectrum at rt can be fitted by two doublets with isomeric shifts of 1.09 and 1.08 mm/s (ratio 1.5:1) which is characteristic of Fe^{2+} ions in the high spin state (Figure 2, Table 1). The different quadrupole splitting of 1.325 and 0.429 mm/s are indicative of different environments of the Fe^{2+} ions either in one common phase or in different ones. A Mößbauer signal, consisting of two doublets with similar isomeric shifts and quadrupole splitting, was observed before for the room temperature orthorhombic phase of Li_2FeCl_4.[28] Unlike in our case the authors found a distinctly different ratio of the two peaks of 6.7 to 1. Moreover, almost five doublets with similar isomeric shifts but different quadrupole splitting were identified in this paper for the room temperature Mößbauer spectrum of the high temperature phase of Li_2FeCl_4.

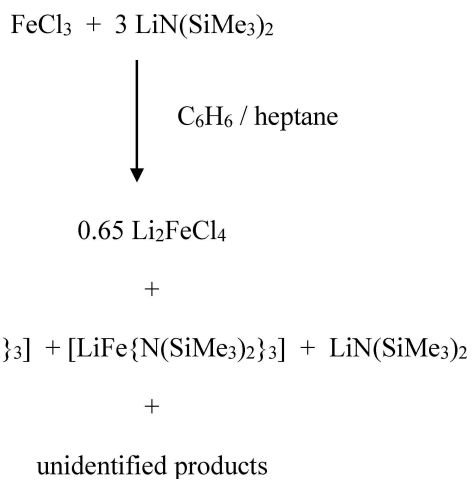

Scheme 1. Synthesis A.

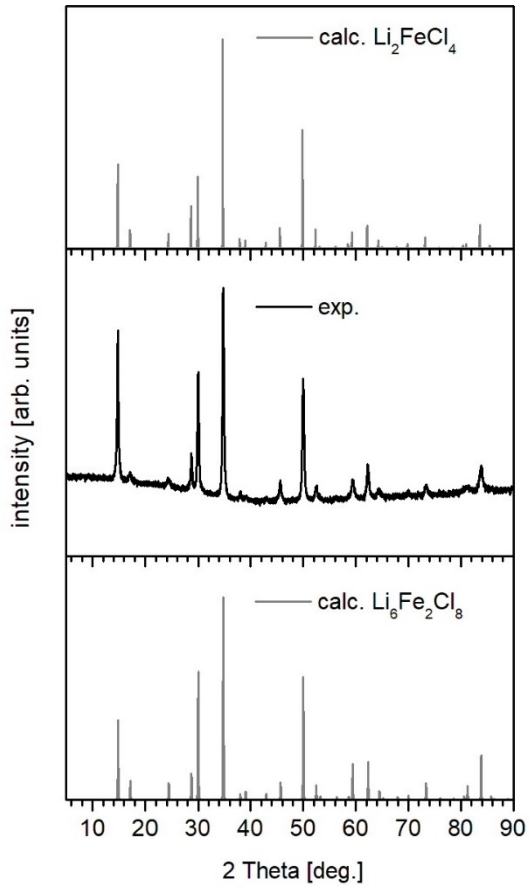

Figure 1. Measured (black) X-ray powder pattern of the solid reaction product of synthesis A (Scheme 1) and simulated (grey) patterns of Li_2FeCl_4[25] (up) and $Li_6Fe_2Cl_8$ (below).[27]

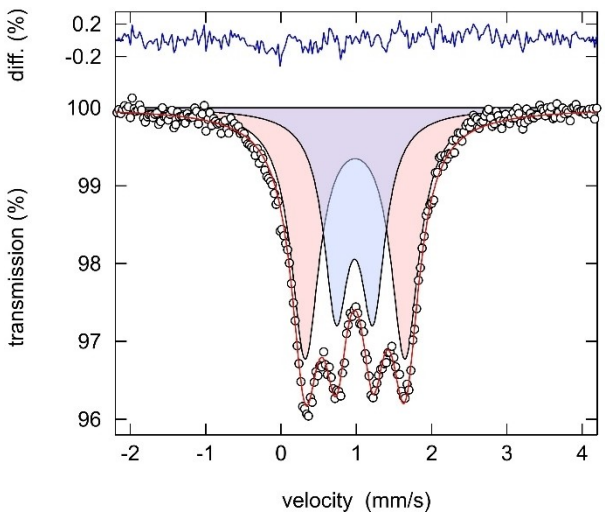

Figure 2. Room temperature ^{57}Fe Mößbauer spectrum of Li_2FeCl_4. Experimental data points are shown as white spheres, the overall fit as a red line, the sub-spectra as blue and red doublets, and the difference plot as blue line.

The findings were rationalized by the fact that the disordered occupation of the octahedrally coordinated metal atoms results

Table 1. Parameters used to fit the ^{57}Fe Mößbauer spectrum of Li_2FeCl_4 (Figure 2).[a,b]

doublet		IS in [mm/s]	QS in [mm/s]	Γ in [mm/s]	area frac.
1	Fe^{2+}	1.090 ± 0.001	1.325 ± 0.004	0.452 ± 0.005	59.3 %
2	Fe^{2+}	1.083 ± 0.001	0.490 ± 0.005	0.398 ± 0.007	40.7 %

[a] Isomer shift IS, Quadrupole splitting QS, line width Γ, and area fraction. [b] IS is given with respect to α-Fe metal at room temperature.

in a different occupation of the six next octahedral places with lithium and iron atoms leading to different field gradients. Different preparation techniques might create different short-range orderings in the structures, which then result in the different splitting and ratios of the peaks. For the related compound Li_6FeCl_8 Lutz et al. reported a ^{57}Fe Mößbauer singlet in agreement with an ideal octahedral coordination environment.[27]

^{6}Li und ^{7}Li MAS NMR of the powder display signals with large paramagnetic shifts (75, 101, 292 ppm) resulting from a close neighborhood of the iron and lithium ions in a common phase via Li–Cl–Fe bonds (Figure 3). Again, the different shifts indicate different second neighborhoods of the lithium atoms as also found for the iron atoms by ^{57}Fe Mößbauer spectroscopy.

The findings clearly indicate the occurrence of redox reactions between oxidizing $FeCl_3$ and reducing $LiN(SiMe_3)_2$ like observed and reported by Putzer et al.[29] and evidenced by a reversible redox transition with the potential of −0,523V ($E_{1/2}$) in the cyclic voltagramm of **1** in thf.[30] The crystallization and especially the isolation of dry crystalline **1** from the dark green supernatant solution of the centrifugation is hampered by the high solubility of **1** (even in small amounts of pentane at −75 °C as already reported by Lee and coworkers[24]) and by the presence of further soluble byproducts as indicated below.

Therefore, we started to sublime the filtrate in vacuum (10^{-3} mbar) after evaporation of the solvent by vacuum distillation. Also for sublimation, the literature information is varying. Bürger and Wannagat reported for **1** a sublimation temperature of 130 °C at 1 Torr.[10] For the product of the 1:3 reaction Bradley and coworkers reported that: 'the dark green product sublimes at 80 °C, 0.005 mmHg with decomposition'.[11] In contrast for **1**, crystallized from a 2:3 reaction a sublimation temperature of 120 °C and 0.005 Torr was reported later on by the same authors.[23] In our case upon increasing the temperature of the oil bath, an almost white (very pale green) sublimate started to form at about 55–60 °C. By further increasing the temperature (up to 100 °C in steps of 5 °C) the colour of the sublimation products then gradually intensifies to dark green. In the upper part of the sublimate the educt $LiN(SiMe_3)_2$[31] and the Fe(II) salt $[LiFe\{N(SiMe_3)_2\}_3]$[32] could be identified by single crystal XRD. In the dark green sublimation product in the lower part of the Schlenk tube no material suitable for single crystal XRD could be identified. Powder XRD of this slightly sticky material in a capillary was possible by mixing it with amorphous glas (Figure 4). The pattern is distinctly different from the simulated one based on the published trigonal structure of $[Fe\{N(SiMe_3)_2\}_3]$[21] in the space

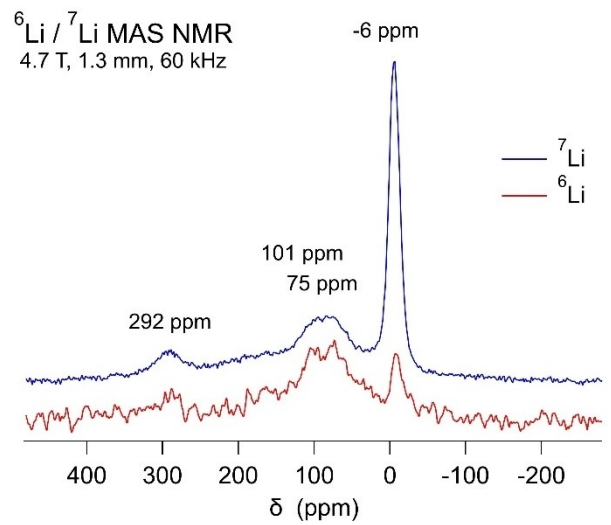

Figure 3. ^{6}Li and ^{7}Li MAS NMR spectra of Li_2FeCl_4.

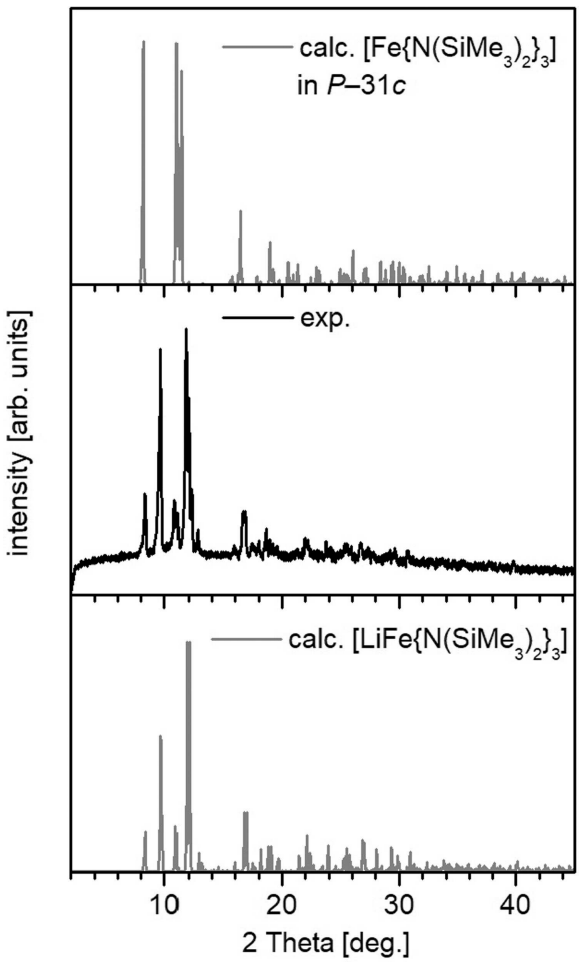

Figure 4. Measured (black) X-ray powder pattern of the dark green sublimation product of the synthesis A (Scheme 1) compared with the simulated (grey) patterns of **1** in $P\bar{3}1c$[22] (up) and $[LiFe\{N(SiMe_3)_2\}_3]$ (below).[32]

group $P\bar{3}1c$ although the dark green colour agrees well with the reported one. Instead, just by visual inspection, the diffractogram looks similar to the one calculated for $[LiFe\{N(SiMe_3)_2\}_3]$ although some of the reflection positions are slightly shifted and more importantly one expects for the latter compound a light green colour.[32] These inconsistencies could be rationalized in the further course of the investigations.

2:3 Reaction of $FeCl_3$ and $LiN(SiMe_3)_2$

In a next step reactions with a 2:3 ratio of iron(III) chloride and the lithium amide were conducted (Scheme 2). Again, powder XRD reveals the formation of a mixed lithium iron chloride salt instead of pure lithium chloride with a powder pattern identical to that of Figure 2. The amount of powder corresponds to ~1.4 equiv. of Li_2FeCl_4.

Crystals of **1** could be obtained upon concentration of the reaction solution. These were identified by single crystal XRD to crystallise in the trigonal space group $P\bar{3}1c$.[21,22]

For reasons already mentioned above, a vacuum sublimation (10^{-3} mbar) of the residue obtained by vacuum condensation of this reaction solution was performed in order to isolate pure **1**. The formation of three main products can be observed. At an oil bath temperature of approximately 50 °C and a pressure of < 1 mbar a small amount of a colorless liquid starts to distill from the dark green residue. At 60 °C a highly viscous film-like green product sublimes followed by the formation of dark green crystals in the Schlenk tube directly above the meniscus of the oil bath when increasing the temperature further from 70 °C to 125 °C. The colorless liquid together with the film-like green product can be separated from the dark green crystals by gentle heating in vacuum.

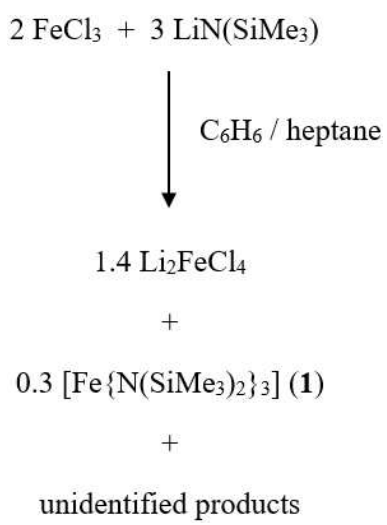

Scheme 2. Synthesis B.

Crystal Structure and Spectroscopic Data of 1

The powder XRD pattern of the dark green crystalline sublimation product is similar to the one of the 1:3 synthesis but in general with narrower reflections (Figure 5). In addition, suitable crystals could be selected for single crystal XRD after a second sublimation, resulting in a new 'solvent-free' structure of **1** crystallizing in the monoclinic space group $P2_1/c$ (Table 2). The molecule is monomeric and three-times coordinated but only of pseudo D_{3h} symmetry (Figure 6). The main bond lengths and angles are almost identical to the ones crystallizing in the trigonal space group $P\bar{3}1c$ (Table 3) and reveal a trigonal planar structure with the iron atom situated in the plane formed by the three nitrogen atoms. Interestingly also the stereochemistry of the molecule, affected by the orientation of the $N(SiMe_3)_2$ groups with respect to the trigonal plane formed by the three nitrogen atoms, is similar (Δ) to the one observed for the solvent containing structure. In summary this means that the cocrystallizing solvents do not have a distinct structural influence on the molecular structure of the tris-amide itself. Related 'solvent-free' structures with a similar crystal metric have been published for $[Al\{N(SiMe_3)_2\}_3]$,[33] $[Ga\{N(SiMe_3)_2\}_3]$[34] and $[Sc\{N(SiMe_3)_2\}_3]$.[16] In the latter one, in contrast to **1**, the metal atom comprises a pyramidal coordination environment being situated ca. 50 pm above the trigonal plane.

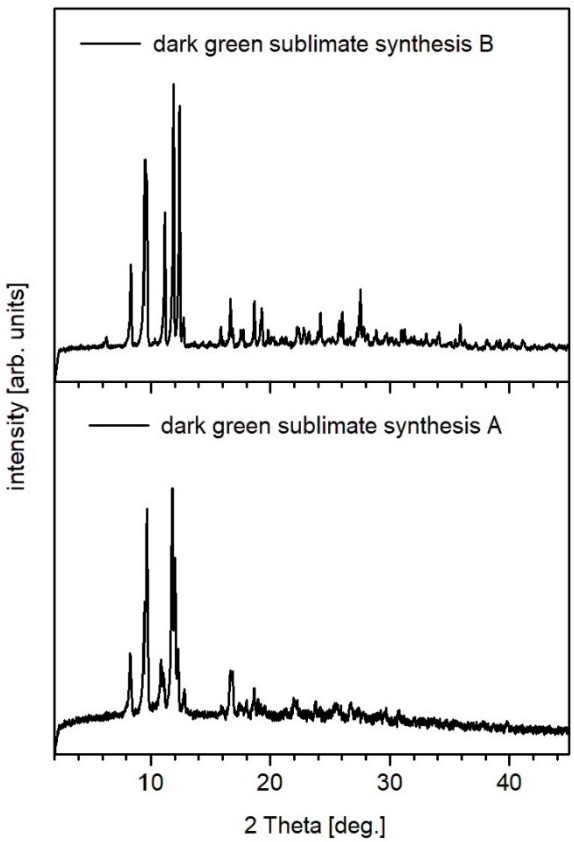

Figure 5. Comparison of the experimental X-ray powder patterns of the dark green sublimation products of synthesis A (below) and B (up) (Scheme 1 and Scheme 2).

Table 2. Crystallographic Data for **1**.

		1
sum formula		$C_{18}H_{54}FeN_3Si_6$
fw [g/mol]		537.03
crystal system		monoclinic
space group		$P2_1/c$
Cell	*a* [Å]	8.4603(17)
	b	20.935(4)
	c	18.420(4)
α		
β		93.30(3)
γ		
V [Å^3]		3257.1(11)
Z		4
T [K]		180(2)
λ [Å]		0.71073
d_c [g cm^{-3}]		1.095
μ(λ) [mm^{-1}]		0.694
F[000]		1172
$2\theta_{max}$ [°]		51
meas reflns		13678
unique reflns		6071
R_{int}		0.0849
reflns with $I > 2\sigma(I)$.		3568
refined params		253
$R1(I > 2\sigma(I))$[a]		0.0447
*wR*2(all data)[b]		0.1252

[a] $R1 = \Sigma||F_o| - |F_c||/\Sigma|F_o|$. [b] $\{\Sigma[w(F_o^2 - F_c^2)^2]/\Sigma[w(F_o^2)^2]\}^{1/2}$.

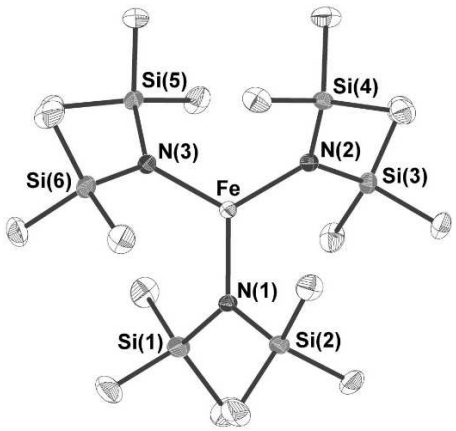

Figure 6. Molecular structure of **1** in the crystal (ellipsoids drawn at 50% probability level, H atoms omitted).

Table 3. Structural parameters in **1** and comparison with values from literature.

	1		
	$P2_1/c$[a]	$P\bar{3}1c$[b]	$P\bar{3}1c$[c]
T [K]	180(2)	rt	150
Fe–N [pm]	189.17(12)	191.7(4)	190.7(1)
	189.42(11)		
	188.44(11)		
N–Si [pm]	174.9–175.1(1)	173.1(3)	174.9(3)
N–Fe–N [°]	120.75(5)	119.4(2)	120.0(1)
	119.34(5)		
	119.91(5)		
Δ_{plane} [d]	0.13(7)		

[a] This work. [b] Data taken from ref. 22. [c] Data taken from ref. 39. [d] Deviation of the metal atom from the trigonal plane [pm].

The measured powder pattern of the dark-green and crystalline sublimation product shows a very good agreement with the calculated one based on the single crystal data as can be seen from the fits performed with the program Fullprof (Figure S1).[35] The elemental analysis of **1** matches the calculated values which is an additional proof of its purity. The yield of **1** obtained by sublimation can be therefore estimated to be 35.5% with respect to the amide which is distinctly lower than those given by Bradley (62%)[23] and Lee (56%)[24] for **1** crystallized from solution.

Interestingly, ^{57}Fe Mößbauer spectroscopy indicates for **1** the existence of an Fe(II) impurity as observed before by others (Figure S2, Table S1).[36] **1** displays a four line spectrum at 77 K which can be fitted as a sum of an outer very asymmetric doublet (relative area 88.5%) and an inner symmetric quadrupole doublet (relative area 11.5%) with the latter one arising from the impurity. Values of the isomeric shift (IS = 0.571 mm·s^{-1}) and quadrupol splitting (QS = 1.213 mm s^{-1}) of this impurity signal are close to the ones found for [Fe{N(SiMe$_3$)$_2$}$_2$]$_2$ on the same instrument at 77 K (IS = 0.586, QS = 1.004 mm s^{-1}) and in literature.[37] In addition the Mößbauer spectrum for the identified Fe(II) reaction byproduct [LiFe{N(SiMe$_3$)$_2$}$_3$] at 77 K (IS = 0.615, QS = 0.904 mm s^{-1}) also turned out to have similar shift and splitting parameters like the impurity signal (Figure S2, Table S1). We note, that the area fractions observed in these Mößbauer spectra are not directly related to molar fractions of the different compounds, since these area fractions depend on the recoil-less fraction as well as the iron mass percentage of the respective compound. Specific recoil-less fractions are accessible only via temperature-dependent measurements.[38]

The clear identification of the impurity compound is complicated by the facts that the lattice constants and crystal packing of [LiFe{N(SiMe$_3$)$_2$}$_3$][32] are quite similar to the structural characteristics of 'solvent-free' **1** crystallizing in $P2_1/c$ which leads to a close similarity (but not identity) of the powder patterns. In addition, values for C, H, N elemental analysis of [LiFe{N(SiMe$_3$)$_2$}$_3$] are almost identical to the corresponding values of **1** and those of [Fe{N(SiMe$_3$)$_2$}$_2$]$_2$ are close. However, in view of the clear indication of a formal oxidation number of two, the impurity compound should rather originate from a decomposition of **1** during the sublimation process or a reaction side product with similar sublimation temperature than from decomposition (hydrolysis/oxidation) of **1** during the Mößbauer measurement.

Compound **1** can be recrystallized from pentane. The powder pattern of the isolated crystals (Figure S3, ESI) reveals that the major phase consists of crystals of the monoclinic form (black needles) which are polymorph (not suitable for single crystal XRD) and only a minor phase is formed by single crystals of the trigonal phase (dark green plates and needles). The Mößbauer spectrum of this material at 77 K is identical to the one of **1** obtained by sublimation (Table S1). Only, the peaks of the Fe^{2+} impurity compound are found to be slightly broader than in the sublimed product.

The UV-Vis NIR spectrum of **1** in THF is almost identical to the one presented by Lee and coworkers (Figure S4, ESI).[24]

However, in comparison to the original data of Bradley and coworkers[12] intensities are found to be 2 to 4 times higher which clearly suggests that the observed bands have to be assigned as ligand to metal charge transfer (LMCT) rather than spin forbidden d-d transitions (Table 4). The spectra of concentrated solutions of **1** do not give evidences for d-d bands in the NIR region characteristic for Fe^{2+} compounds[8,9] which additionally indicates (in line with powder XRD and elemental analysis) that the amount of contamination, proven by Mößbauer spectroscopy, must be low.

DC and AC Magnetic Properties of 1

The static and dynamic magnetic properties of **1** crystallized from toluene were published in a recent paper.[39] For comparison, we performed dc magnetic measurements of **1**, obtained by sublimation, between 2 and 300 K in a field of 0.1 T and magnetization measurements from 0 to 7 T at 2, 3, 4, 6, 10 and 25 K. Similar to the results of Ge et al. the values of χT display a clear deviation from the Curie law below 30 K and, in agreement, the shape of the magnetization curves indicates magnetic anisotropy (Figure S5 and Figure S6, ESI).[39] However, fits of our data performed with the PHI program[40] lead to slightly different spin Hamiltonian (SH) parameters given and compared in Table 5 (satisfying fits could not be obtained with an isotropic *g* value). The model includes both axial (*D*) and rhombic (*E*) zero field splitting (ZFS) terms as well as Zeeman interactions with an anisotropic treatment of *g* (eqn (S1), ESI). Also in our case the data of the powdered samples lead to fits of similar quality for negative or positive *D* parameters. Ge et al. determined the sign of *D* by high frequency electron paramagnetic resonance (HFEPR) measurements to be negative in agreement with early results from EPR measurements obtained by Bradley and coworkers.[41]

Field dependent ac measurements[42] were performed at 2 K using a 3.0 Oe ac field, oscillating at an extended range of frequencies between 10 and 10000 s^{-1} and compared with measurements published in ref. 39 (Figure S7, ESI). In the absence of an external dc field ($H_{dc}=0$), the out-of-phase component of the ac susceptibility (χ'') of **1** has much lower intensity than the in-phase component (χ') and displays no maximum. However, at higher frequencies a spin-lattice relaxation process which is slightly faster than the timescale of the experiment is indicated by an increase of χ''. With the application of a static dc field (H_{dc} up to 5000 Oe), the intensity of χ'' is significantly enhanced and the maximum is shifted to lower frequencies. Relaxation times τ of the relaxation processes at a given temperature and field were derived from simultaneous fits of the frequency dependent curves of χ' and χ'' vs ν according to eqn S2 and S3. The resulting field dependence of the inverse relaxation time at 2 K displays a curvature feature with a minimum around 2500-3000 Oe and a negative slope for smaller and a positive slope for larger fields (Figure S8, ESI). This behaviour can be approximately fitted by using eqn. (S4) similar to a previous approach.[43]

At an external field of 2500 Oe the plot of $\ln\tau$ against the reciprocal temperature (derived from temperature dependent ac measurements) follows almost a straight line in the region from 2 to 4 K indicating a dominant Arrhenius type Orbach relaxation process (Figure S9–S11, ESI). Corresponding fits to eqn S5 yielded an energy barrier to the thermal reversal of the magnetic moment U_{eff} of about 7.4 cm^{-1} ($\tau_0 = 9.1\cdot10^{-7}$ s^{-1}). The value of U_{eff} is quite similar to the one obtained by Ge et al. ($U_{eff} = 6.91$ cm^{-1}) from ac measurements at $H_{dc} = 1600$ Oe on crystals obtained by crystallization from solution.[39] In contrast, the pre-exponential factor for those crystals is higher by one order of magnitude ($\tau_0 = 3.85\cdot10^{-5}$ s^{-1}) when compared with our data for the 'solvent-free' crystals obtained by sublimation (In this context we note that most probably this number in literature is wrong by one order of magnitude and should read $\tau_0 = 3.85\cdot10^{-6}$ s^{-1} fitting better to the graph and which would then mean a much better agreement with our results).

In order to get additional information about the spin relaxation processes in **1** it was magnetically diluted with 2 equivalents of $[Al\{N(SiMe_3)_2\}_3]$ by a combined vacuum sublimation. The resulting product of formal composition $[FeAl_2\{N(SiMe_3)_2\}_9]$ was structurally characterized by powder XRD (Figure S12, Table S2, ESI). The lattice constants obtained by fits with the FullProf program[35] show a continuous trend from the pure aluminium containing compound to **1** (decreasing *a* and increasing *b*, *c* and β). This can be viewed as an indication for mixing of the two species in the crystal lattice at the molecular level.

DC magnetic measurements show only slight differences from the data measured for **1** (Figure S13, ESI). AC magnetic measurements reveal a general shift of the χ'' vs ν maxima to lower frequencies in comparison to the pure iron compound **1** (Figure S14–S17, ESI). For example, the onset of the signal in zero field becomes now clearly visible at higher frequencies

Table 4. UV-Vis NIR data of **1** in thf and comparison to the values from literature.[12]

this work thf		lit. values cyclohexane	
λ [nm]	ε [L mol^{-1} cm^{-1}]	λ [nm]	ε [L mol^{-1} cm^{-1}]
351(sh)	4006	336	1500
406	5550	395	1500
494(sh)	1727	500	400
633	1846	621	450

Table 5. The SH parameters of **1** extracted from a simultaneous PHI simulation of the dc magnetic data (eqn (S1) and Figure S2 and Figure S3) and compared to literature values.[39]

	1[a] $P2_1/c$		**1**[b] $P\bar{3}1c$	
D [cm^{-1}]	−1.43	1.46	−1.48	1.67
E/D	0.469	0.233	< 0.01	0.25
g_x	2.159	1.973	$g_{iso} = 1.871$	$g_{iso} = 1.879$
g_y	2.092	1.973		
g_z	1.839	2.110		
TIP [cm^{3}mol^{-1}]	5.6E-4	7.7E-4	not given	
R	99.99812	99.99835		

[a] This work. [b] Ref. 39.

with an estimated maximum around 11000 s^{-1}. Maxima at H_{dc} = 2500 Oe (T = 2 K) amount to 840 s^{-1} for **1** in comparison to 416 s^{-1} for the mixed complex $[FeAl_2\{N(SiMe_3)_2\}_9]$.

Despite this obvious shift, an evaluation of the field, temperature and frequency dependent ac data of $[FeAl_2\{N(SiMe_3)_2\}_9]$ revealed only slight changes of the parameters characteristic for the relaxation process in comparison to **1** ($\tau_0 = 1.38(1)\cdot10^{-6}$ s^{-1}, U_{eff} = 7.8(1) cm^{-1}).

Therefore, in comparison with the ac data of Ge et al., it seems for **1** to be the case that an inclusion of lattice solvent molecules or a dilution with diamagnetic isostructural molecules induces a shift of the absolute frequency of the respective relaxation process to lower frequencies but does not affect U_{eff} or τ_0. This indicates that the energy barrier itself is a molecular property of **1** whereas the absolute frequency of the relaxation process is additionally determined by the properties of the crystal lattice.

Conclusion

A new 'solvent-free' crystal structure was identified for crystals of $[Fe\{N(SiMe_3)_2\}_3]$ isolated by vacuum sublimation of the soluble products of the reaction of 2 $FeCl_3$ and 3 $LiN(SiMe_3)_2$ in arene solvents. In addition we found, in line with notes in previous papers,[10,24] clear evidences that both, the more intuitive '1:3 reaction protocol', as well as this synthesis suffer from redox reactions, which lead to a number and distinct amount of byproducts complicating the isolation of the target compound and reducing its theoretical yield. Ac magnetic data of magnetically diluted samples of $[Fe\{N(SiMe_3)_2\}_3]$ reveal an influence of the properties of the crystal lattice (inclusion of solvents or dilution with isostructural nonmagnetic molecules) on the absolute frequency of the relaxation process.

Experimental Section

Standard Schlenk techniques were employed throughout the syntheses using a double-manifold vacuum line with high-purity dry nitrogen (99.9994%) and an MBraun glovebox with high-purity dry argon (99.9990%). The solvents hexane and pentane were dried over $LiAlH_4$, diethyl ether over sodium-benzophenone and both distilled under nitrogen. $LiN(SiMe_3)_2$ and anhydrous $FeCl_3$ were purchased from Aldrich. $LiN(SiMe_3)_2$ was distilled prior to use. $[LiFe\{N(SiMe_3)_2\}_3]$ was synthesized according to literature.[32]

Synthesis A ('1:3'): 3 equivalents of $LiN(SiMe_3)_2$ (1.55 g, 9.25 mmol) were dissolved in a mixture of 10 mL benzene and 10 mL hexane. In between 30 min, 1 equivalent of solid $FeCl_3$ (0.5 g, 3.08 mmol) were added in small portions to this stirred solution to give a dark green solution. After stirring overnight and brief gentle heating with a heat gun the precipitate was separated by centrifugation from the solution and washed once with benzene and once with Et_2O to give 435 mg of an almost white powder. The decanted dark green solution was reduced to dryness by vacuum condensation and then this residue heated under vacuum (10^{-3} mbar). At an oil bath temperature of 60–65 °C an almost white (very pale green) sublimate started to form. By further increase of the temperature (100 °C in steps of 5 °C) the colour of the sublimation products then gradually intensifies to dark green with the pale green zone moving up.

Synthesis B ('2:3'), $[Fe\{N(SiMe_3)_2\}_3]$ (**1**): 3 equivalents of $LiN(SiMe_3)_2$ (1.55 g, 9.25 mmol) were dissolved in a mixture of 10 mL benzene and 10 mL hexane. In between 30 min, 2 equivalents of solid $FeCl_3$ (1 g, 6.16 mmol) were added in small portions to this stirred solution to give a dark green solution. After stirring overnight and brief gentle heating with a heat gun, the precipitate was separated by centrifugation from the solution and washed once with benzene and once with Et_2O to give 435 mg of an almost white powder. The decanted dark green solution was reduced to dryness by vacuum condensation and then this residue was heated under vacuum (10^{-3} mbar). At an oil bath temperature of 55–60 °C an intense green and film-like product forms in the upper part of the Schlenk tube. At a bath temperature of approximately 85 °C dark green crystals started to form right above the meniscus of the oil. Now, the products in the upper part were transferred by gentle heating with a heat gun to a connected Schlenk tube. Then the temperature of the bath was increased stepwise to 125 °C and kept until no more formation of sublimation products was observed. If more of the intense green and film-like product has been formed it was again removed in the way described before. After cooling, 590 mg (35,5% based on amide) of dark green **1** could be isolated from the wall of the Schlenk tube in a glove box. 500 mg of **1** obtained from sublimation were recrystallized from 4 mL of pentane at 25–30 °C. The crystals were washed once with 4 mL of cold pentane (−78 °C) and then quickly dried in vacuum to give 340 mg of **1**. Even at these low temperatures **1** is distinctly soluble in pentane.

(**1**) $C_{18}H_{54}FeN_3Si_6$ (537): calcd C 40.3, H 10.1, N 7.8 found C 40.5, H 10.5, N 7.7%.

Crystallography

Due to the air and moisture sensitivity of the compounds, crystals suitable for single crystal X-ray diffraction were selected in perfluoroalkylether oil in a glove box and transferred rapidly under argon atmosphere to the diffractometer equipped with an Oxford Cryosystem. Single-crystal X-ray diffraction data of **1** were collected using graphite-monochromatised Mo-K_α radiation (λ = 0.71073 Å) on a STOE IPDS II (Imaging Plate Diffraction System). Raw intensity data were collected and treated with the STOE X-Area software Version 1.64. Data for all compounds were corrected for Lorentz and polarisation effects. Based on a crystal description a numerical absorption correction was applied for.[44] The structure was solved with the direct methods program SHELXS of the SHELXTL PC suite programs,[45] and was refined with the use of the full-matrix least-squares program SHELXL. The molecular diagram was prepared using Diamond.[46]

In **1** all Fe, Si, N, and C atoms were refined with anisotropic displacement parameters whilst H atoms were computed and refined, using a riding model, with an isotropic temperature factor equal to 1.2 times the equivalent temperature factor of the atom which they are linked to.

X-ray powder diffraction patterns (XRD) (powder of crystals), were measured at rt on a STOE STADI P diffractometer (Cu-$K_{\alpha1}$ or Co-$K_{\alpha1}$ radiation, Germanium monochromator, Debye-Scherrer geometry, Mythen 1 K detector) in sealed glass capillaries. The theoretical powder diffraction patterns were calculated on the basis of the atom coordinates obtained from single crystal X-ray analysis (180 K) by using the program package STOE WinXPOW.[47]

The experimental pattern of **1** was fitted with the FullProf program[35] using the atom coordinates from single crystal data. Main refinement parameters were: cell parameters, scale factor,

zero-shift, background, overall temperature factor and coordinates of the Fe, Si, and N atoms. Profile parameters for a pseudo Voigt profile with axial broadening were used.[48,49]

Physical Measurements

C, H, S elemental analyses were performed on an 'Elementar vario Micro cube' instrument.

UV-Vis absorption spectra were measured on a Perkin Elmer Lambda 900 spectrophotometer in quartz cuvettes.

^{6}Li and ^{7}Li MAS NMR measurements were performed on a Bruker Avance 200 MHz spectrometer at a magnetic field of 4.7 T, corresponding to Larmor frequencies of 29.4 MHz (^{6}Li) and 77.8 MHz (^{7}Li). Spinning was performed in 1.3 mm rotors at 60 kHz. Spectra were acquired with a rotor-synchronized Hahn-echo pulse sequence with a $\pi/2$ pulse length of 0.9 μs and a recycle delay of 5 s. Spectra are referenced to aqueous solutions of LiCl or ^{6}LiCl at 0 ppm.

Fe Mößbauer spectroscopy was performed with a constant-acceleration spectrometer at room temperature in transmission mode with a ^{57}Co(Rh) source. Isomer shifts are given relative to that of α-Fe metal. Powder samples were sealed in polyethylene bags in an argon-filled glove box to avoid contact with air.

Zero-Field-Cooled temperature dependent susceptibilities were recorded in dc mode using a MPMS-III or MPMS-XL (Quantum Design) SQUID magnetometer over a temperature range from 2 to 300 K in a homogeneous 0.1 T external magnetic field. The magnetization curves were measured on the same instrument up to a dc field of 7 T. The ac susceptibility measurements have been performed using a PPMS (Quantum Design) Dynacool magnetometer with an oscillating ac field of 3 Oe and ac frequencies ranging from 10 to 10000 Hz. The samples were contained in gelatine capsules filled in a glove box under argon atmosphere owing to the high degree of moisture and oxygen sensitivity of the compounds. The samples were transferred in sealed Schlenk tubes from the glove box to the magnetometer and then rapidly transferred to the helium-purged sample space of the magnetometer. The data were corrected for the sample holder including the gelatine capsule and for diamagnetism using Pascal's constants.[50,51,52]

Deposition Number 1966421 (for **1**) contains the supplementary crystallographic data for this paper. These data are provided free of charge by the joint Cambridge Crystallographic Data Centre and Fachinformationszentrum Karlsruhe Access Structures service www.ccdc.cam.ac.uk/structures.

Supporting information

(see footnote on the first page of this article): Details about the simulations are given in the ESI.

Author Contributions

S. Indris: Li MAS NMR and Mößbauer spectroscopy, M. Knapp: Fullprof Rietveld refinements, B. Schwarz: magnetic ac measurements, A. Eichhöfer: synthesis and characterization,

Acknowledgements

This work was supported by the Karlsruhe Institut für Technologie (KIT, Campus Nord) and the Karlsruhe Nano-Micro-Facility (KNMF). The authors thank S. Stahl for the performance of the elemental analysis and V. Mereacre and S. Abhishek for performance of low temperature Mößbauer measurements. A. E. thanks A. K. Powell for generous support. Open access funding enabled and organized by Projekt DEAL.

Conflict of Interest

The authors declare no conflict of interest.

Keywords: iron · amides · Fe-Mößbauer spectroscopy · Li-NMR spectroscopy · magnetic properties

[1] P. P. Power, *Chem. Rev.* **2012**, *112*, 3482–3507.
[2] P. P. Power, *Chemtracts* **1994**, *6*, 181–194.
[3] M. F. Lappert, P. P. Power, A. R. Sanger, R. C. Srivastava, *in Metal and Metalloid Amides*, ed. by E. Horwood, Chichester, **1980**.
[4] T. Nguyen, A. Panda, M. M. Olmstead, A. F. Richards, M. Stender, M. Brynda, P. P. Power, *J. Am. Chem. Soc.* **2005**, *127*, 8545–8552.
[5] A. Eichhöfer, O. Hampe, S. Lebedkin, F. Weigend, *Inorg. Chem.* **2010**, *49*, 7331–7339.
[6] A. Eichhöfer, G. Buth, *Eur. J. Inorg. Chem.* **2019**, 639–646.
[7] P.-H. Lin, N. C. Smythe, S. I. Gorelsky, S. Maguire, N. J. Henson, I. Korobkov, B. L. Scott, J. C. Gordon, R. T. Baker, M. Murugesu, *J. Am. Chem. Soc.* **2011**, *133*, 15806–15809.
[8] A. Eichhöfer, Y. Lan, V. Mereacre, T. Bodenstein, F. Weigend, *Inorg. Chem.* **2014**, *53*, 1962–1974.
[9] T. Bodenstein, A. Eichhöfer, *Dalton Trans.* **2019**, *48*, 15699–15712.
[10] H. Bürger, U. Wannagat, *Monatsh. Chem.* **1963**, *94*, 1007–1012.
[11] E. C. Alyea, D. C. Bradley, R. G. Copperthwaite, *J. Chem. Soc. Dalton Trans.* **1972**, 1580–1584.
[12] E. C. Alyea, D. C. Bradley, R. G. Copperthwaite, K. D. Sales, *J. Chem. Soc. Dalton Trans.* **1973**, 185–191.
[13] D. C. Bradley, R. G. Copperthwaite, S. A. Cotton, K. D. Sales, *J. Chem. Soc. Dalton Trans.* **1973**, 191–194.
[14] P. G. Eller, D. C. Bradley, M. B. Hursthouse, D. W. Meek, *Coord. Chem. Rev.* **1977**, *24*, 1–95.
[15] J. S. Ghotra, M. B. Hursthouse, A. J. Welch, *J. Chem. Soc. Chem. Commun.* **1973**, 669.
[16] D. H. Woen, G. P. Chen, J. W. Ziller, T. J. Boyle, F. Furche, W. J. Evans, *Angew. Chem. Int. Ed.* **2017**, *56*, 2050–2053; *Angew. Chem.* **2017**, *129*, 2082–2085.
[17] M. A. Putzer, J. Magull, H. Goesmann, B. Neumüller, K. Dehnicke, *Chem. Ber.* **1996**, *129*, 1401–1405.
[18] C. L. Wagner, N. A. Phan, J. C. Fettinger, L. A. Berben, P. P. Power, *Inorg. Chem.* **2019**, *58*(9), 6095–6101.
[19] R. D. Köhn, G. Kociok-Köhn, M. Haufe, *Chem. Ber.* **1996**, *129*, 25–27.
[20] J. J. Ellison, P. P. Power, S. C. Shoner, *J. Am. Chem. Soc.* **1989**, *11*, 8044–8046.
[21] D. C. Bradley, M. B. Hursthouse, R. F. Rodesiler, *J. Chem. Soc. Chem. Commun.*, 1969, 14–15.
[22] M. B. Hursthouse, P. F. Rodesiler, *J. Chem. Soc. Dalton Trans.* **1972**, 2100–2102.
[23] D. C. Bradley, R. G. Copperthwaite, *Inorg. Synth.* **1978**, *18*, 112–120.
[24] J. S. Duncan, T. M. Nazif, A. K. Verma, S. C. Lee, *Inorg. Chem.* **2003**, *42*, 1211–1224.
[25] R. Kanno, Y. Takeda, A. Takahashi, O. Yamamoto, *J. Solid State Chem.* **1988**, *73*, 363–375.
[26] H. D. Lutz, A. Pfitzner, J. K. Cockcroft, *J. Solid State Chem.* **1993**, *107*, 245–249.
[27] E. Riedel, D. Prick, A. Pfitzner, H. D. Lutz, *Z. Anorg. Allg. Chem.* **1993**, *619*, 901–904.

[28] H. D. Lutz, A. Pfitzner, W. Schmidt, E. Riedel, D. Prick, *Z. Naturforsch.* **1989**, *44*a, 756–758.
[29] M. A. Putzer, B. Neumüller, K. Dehnicke, J. Magull, *Chem. Ber.* **1996**, *129*, 715–719.
[30] M. G. Margraf, F. Schödel, I. Sänger, M. Bolte, M. Wagner, H.-W. Lerner, *Z. Naturforsch.* **2012**, *67b*, 549–556.
[31] R. D. Rogers, J. L. Atwood, R. Grüning, *J. Organomet. Chem.* **1978**, *157*, 229–237.
[32] S. N. König, D. Schneider, C. Maichle-Mössmer, B. M. Day, R. A. Layfield, R. Anwander, *Eur. J. Inorg. Chem.* **2014**, 4302–4309.
[33] J. A. Tang, J. D. Masuda, T. J. Boyle, R. W. Schurko, *ChemPhysChem* **2006**, *7*, 117–130.
[34] S Kuhner, R. Kuhnle, H.-D. Hausen, J. Weidlein, *Z. Anorg. Allg. Chem.* **1997**, *623*, 25–34.
[35] J. Rodrıguez-Carvajal, *Physica B + C*, **1993**, *192*, 55–69.
[36] B. W. Fitzsimmons, C. E. Johnson, *Chem. Phys. Lett.* **1974**, *24*, 422–424.
[37] D. J. Evans, D. L. Hughes, J. Silver, *Inorg. Chem.* **1997**, *36*, 747–748.
[38] G. K. Shenoy, F. E. Wagner (Eds.), *Mössbauer Isomer Shifts*, North-Holland Publishing Company, Amsterdam, **1979**.
[39] N. Ge, Y.-Q. Zhai, Y.-F. Deng, Y.-S. Ding, T. Wu, Z.-X. Wang, Z. Ouyang, H. Nojiri, Y. Z. Zheng, *Inorg. Chem. Front.* **2018**, *5*, 2486–2492.
[40] N. F. Chilton, R. P. Anderson, L. D. Turner, A. Soncini, K. S. Murray, *J. Comput. Chem.* 2013, **34**, 1164–1175.
[41] D. C. Bradley, R. G. Copperthwaite, S. A. Cotton, K. D. Sales, J. F. Gibson, *Dalton Trans.* **1973**, 191–194.
[42] C. V. Topping, S. J. Blundell, *J. Phys. Condens. Matter*, **2019**, *31*, 013001 (27pp).
[43] M. Zadrozny, M. Atanasov, A. Bryan, C.-Y. Lin, B. D. Rekken, P. P. Power, F. Neese, J. R. Long, *Chem. Sci.* **2013**, *4*, 125–138.
[44] X-RED32 1.01, Data Reduction Program, Stoe & Cie GmbH, Darmstadt, Germany, 2001.
[45] G. M. Sheldrick, SHELXTL PC version 5.1 An Integrated System for Solving, Refining, and Displaying Crystal Structures from Diffraction Data, Bruker Analytical X-ray Systems, Karlsruhe, **2000**.
[46] K. Brandenburg, Diamond Version 2.1d„ Crystal Impact GbR, 1996–2000.
[47] STOE, WinXPOW, STOE & Cie GmbH, Darmstadt, **2000**.
[48] P. Thompson, D. E. Cox, J. B. Hastings, *J. Appl. Crystallogr.* **1987**, *20*, 79–83.
[49] L. W. Finger, D. E. Cox, A. P. Jephcoat, *J. Appl. Crystallogr.* **1994**, *27*, 892–900.
[50] O. Kahn, *Molecular Magnetism*, Wiley-VCH, Weinheim **1993**.
[51] H. Lueken, *Magnetochemistry*, B. G. Teubner, Stuttgart, Leibzig **1999**, p. 426.
[52] W. Haberditzl, *Angew. Chem. Int. Ed. Engl.* **1966**, *5*, 288–323.

Manuscript received: November 19, 2020
Revised manuscript received: January 5, 2021